

Force and Motion Measurements of a Passively Oscillating Hydrofoil

M. N. Mumtaz Qadri, H. Tang and Y. Liu

Department of Mechanical Engineering
The Hong Kong Polytechnic University, Kowloon, Hong Kong, China

Abstract

Energy extraction using flapping foils is a novel concept in the field of renewable energy, especially when the system's locomotion is fully passive and solely dependent on fluidic forces. In order to investigate this concept, a water-tunnel test rig was designed and fabricated in such a way that a hydrofoil is able to periodically heave and pitch under hydrodynamic forces. Energy extraction performance was investigated systematically through simultaneous measurements of the hydrofoil's two degree-of-freedom (DoF) motions and hydrodynamic forces/torques, at two flow velocities (corresponding to the Reynolds Number (Re) $\approx 0.9 \times 10^5$ and 1.1×10^5). This study is focused on the effect of maximum pitching angle of the hydrofoil on the performance of the system. Hydrodynamic forces, extracted power and efficiencies were measured and calculated to evaluate the system performance at three maximum pitching angles. It was observed that increasing the free-stream velocity increased the energy extraction efficiency and power output of the system. Also, a peak appears in average power coefficient and efficiency when the maximum pitching angle is at the intermediate value.

Introduction

In past years, tidal stream energy converters have become a focus for renewable energy research and a majority of the existing designs utilize either horizontal-axis or vertical-axis turbines, which present many challenges related to economic and technical viability [12]. These conventional rotary turbines rely on the flow remaining smoothly attached to the blades for higher power output and efficiency. However, in contrast to the flapping foils seen in nature they have been shown to generate higher instantaneous forces by allowing the flow to separate near the foil's leading edge in the form of a leading edge vortex (LEV) and exploiting the low pressures in the vortex core [11]. Such techniques are used by insects to create high lift from relatively small wings [11], up to four times the lift achievable by a fixed-wing aircraft, and by marine animals to generate large propulsive and manoeuvring forces. Therefore, it is natural to consider flapping motions as an alternative to rotary designs and to explore whether this new concept can help achieve higher power generation and efficiency than conventional systems.

The application of flapping foils in extracting energy from uniform flow was first proposed by McKinney & DeLaurier [8]. Further experimental and numerical investigations have also been conducted in detail by Jones and Platzer [3], Jones et al.[4], Kinsey and Dumas [5][6][7], Zhu and Peng [14], and Xiao et al [13].

Past investigations show that a flapping motion can vary from the propulsion mode to the energy extraction mode if the wing pitches at an angle exceeding its heave induced angle of attack [3]. A recent research by Xiao et al [13] also revealed that an appropriately proposed non-sinusoidal pitch trajectory can effectively enhance device efficiency by tuning the instantaneous angle of attack to a favourable profile. This analysis has been

thoroughly investigated numerically by Ashraf [1] and experimentally by Fenercioglu [2] using a flat plate. However, in the latter study, both pitch and plunge motions were prescribed by the use of actuators.

In this study, we experimentally investigate the effect of varying the maximum pitching angle of the hydrofoil on the hydrodynamic performance of a passively oscillating energy extraction device in open-channel flow at two different flow velocities.

Experimental Setup

Test Facility & Rig Design

The experimental study was carried out in a closed-circuit water channel, which has cross-sectional dimensions of $0.3 \text{ m} \times 0.6 \text{ m}$ and length 2.0 m. Flow speeds can be adjusted between 0.05 m/s and 4 m/s. Using an LDA system, the free-stream turbulence intensity of the water tunnel was found to be about 3%.

The design of the test rig is shown in figure 1. It is inspired from the design of an oscillating wing energy harvester by Platzer et al. [9]. Slight modifications were made to the standard design used for experiments by Semler [10] to accommodate the sensors for dynamic measurements. The hydrofoil in this study is made of aluminium with a rectangular planform of chord length (c) of 140 mm and span (s) of 200 mm and mounted in a vertical cantilevered arrangement in the water oscillating about pivot location $x_p = 0.65c$. To maintain the two dimensionality of the study, end-plates made from acrylic sheets were introduced on the top and bottom of the hydrofoil in the water tunnel test section.

A six-component ATI Mini-40 IP68 Force/Torque (F/T) sensor (ATI Industrial Automation, Inc.) was used to measure the forces and moments on the flapping hydrofoil. The sensor was attached to the vertical cantilevered arrangement between the flat plate model and the main aluminium platform, oriented with its cylindrical z -axis normal to the pitch-heave plane. To measure the rotary and linear kinematic parameters, a Kubler Sendix 5020 Push-Pull configuration rotary incremental encoder and a Type 4382 V uni-axis charge accelerometer from Bruel & Kjaer were used respectively.

All sensors are connected to a computer via a National Instrument (NI) cDAQ 9174 Compact DAQ chassis which houses three different DAQ modules interfaced with the three sensors: two analogue input modules (NI 9220 for the ATI force sensor and NI 9215 for the charge accelerometer) and one digital input module (NI 9411 for the rotary incremental encoder). Dynamic force, moment, linear displacement and rotary displacement data were collected using Labview VI (Virtual Instrument) for approximately 100~110 cycles with a sampling rate of 2000 Hz. Although, data from the analogue sensors could be collected at a much higher sampling rate, the VI block for the digital rotary encoder limited the amount of sampling frequency used. Hence to maintain consistency, real time data acquired from all sensors was kept the same. The first and last 25 cycles

were chopped off and force/moment and kinematic data were phase averaged over 50 cycles. Using an in-house Matlab code, linear and angular velocity and acceleration were calculated and a low pass FFT filter with a cut-off frequency of 10 Hz, which is 12 times higher than the highest flapping frequency, was applied to remove high-frequency noise. At the end, the data set containing nine parameters were phase averaged and analysed.

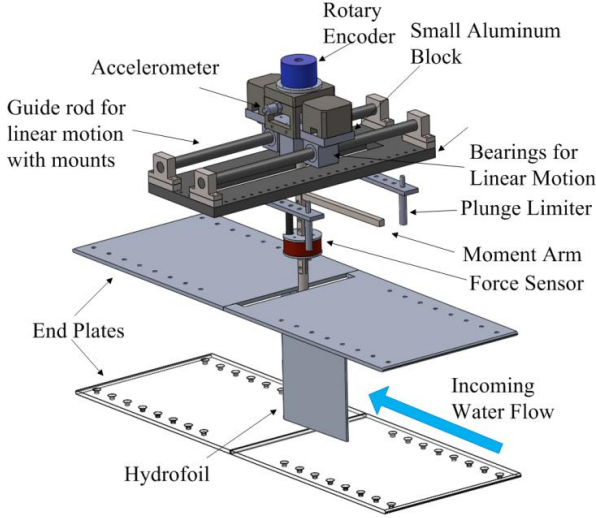


Figure 1. Experimental setup of a passively oscillating energy harvester with sensors and endplates installed.

Since the force/torque sensor rotates with the model undergoing pitch and heave motions, the lift force (F_v) and drag force (F_H) were calculated by resolving the measured forces (F_x and F_y). The z -axis of the force sensor was already in the span-wise direction, hence no transformations of moment (T_z) data were required. Since the acquisition of all sensor data was synchronized in the LabView program, the instantaneous angular displacement data was used to resolve the force data. Later on inertial forces ($F_{inertial}$) and ($T_{inertial}$) were subtracted from lift force and moment data to get net lift force ($F_{v-hydro}$) and net moment ($T_{z-hydro}$).

Motion Kinematics & System Performance Parameters

Figure 2 shows the kinematics of the passively oscillating hydrofoil along with real-time images captured using a video mode of Canon EOS 70D digital camera with frame resolution of 1920×1080 at 23 frames/sec. It is seen that the flapping hydrofoil performs two motions, i.e. heave and pitch. When the water speed is above the cut-off velocity (i.e. $U_{o-cut-off} = 0.68$ m/s), the hydrofoil starts to move due to the action of the hydrodynamic forces. These forces rotate (pitching) the hydrofoil until it is stopped by a pitching angle mechanical restraint. This, in turn, moves the small aluminium block as shown in figure 1, with which the hydrofoil is connected via a vertical shaft. The hydrofoil slides (heaves) on the guide rod due to the lift force generated by the hydrodynamic forces on the hydrofoil, and then the foil is flipped back down at the end of the stroke by the moment arm coming in contact with the heave limiter (figure 1). The hydrofoil rotates in the opposite direction allowing the hydrodynamic forces to translate the foil in the opposite direction and the cycle repeats with continuous upstroke and downstroke motions (figure 2).

The test-rig is a fully passive device and does not consist of any elaborate mechanical mechanisms to enforce proper phase angle between pitch and motions or to create a prescribed non-sinusoidal or sinusoidal pitch motion. The time histories of the linear and rotary kinematics are purely dependent on the hydrodynamic forces from the incoming water flow.

Post-processed force and moment data and linear and angular kinematics data acquired from the sensors in real-time are used to evaluate the system performance of this new flow energy extractor. The instantaneous extracted power P (equation(1)), power coefficient C_p (equation(2)), time-averaged power coefficient \bar{C}_p (equation(3)) and power conversion efficiency η (equation(4)) expressions are used to assess the system's energy harvesting performance.

$$P = F_v \dot{y} + T_z \dot{\theta} \quad (1)$$

where lift F_v , moment T_z , heave motion \dot{y} and pitch motion $\dot{\theta}$ are as depicted in figure 2.

$$C_p = C_v \frac{\dot{y}}{U_o} + C_z \frac{\dot{\theta}}{U_o} \quad (2)$$

$$\bar{C}_p = \frac{1}{T} \int_t^{t+T} C_p(t) dt \quad (3)$$

where $C_v (=F_{v-hydro}/(0.5\rho U_o^2 sc))$ and $C_z (=T_{z-hydro}/(0.5\rho U_o^2 sc^2))$. The efficiency of power generation is measured as the ratio of time-averaged power output to the available power in the flow through the frontal area of the foil:

$$\eta = \frac{\bar{P}}{\frac{1}{2} \rho U_o^3 s d} = \bar{C}_p \frac{c}{d} \quad (4)$$

where d is the largest distance swept by any portion of the foil (usually the trailing edge) as shown in figure 2.

It should be noted that the experimental setup does not include any kind of power take-off (PTO) device for the evaluation of the system's actual energy extraction performance. For convenience, although it cannot fully represent the converted electrical energy, in the present study the hydrofoil's mechanical energy (calculated using the measured hydrodynamic forces and motions as formulated in equations (1)) is used to evaluate the capability of the system in extracting energy from the water flow.

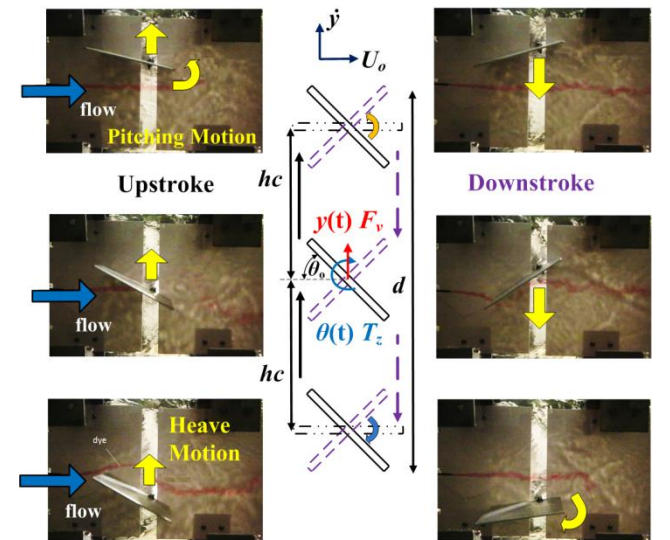


Figure 2. Kinematics of the passively oscillating hydrofoil.

Results and Discussion

This paper focuses on the performance of flapping foil energy harvester at three maximum pitch angles, i.e. $\theta_{o-max} = 30^\circ, 43^\circ$ and 60° , and two free stream velocities, i.e. $U_o = 0.72$ m/s and 0.79 m/s.

Figure 3 shows the variations of the hydrofoil's linear and angular displacements at the three maximum pitch angles. With reference to figure 1, the limit set for translational motion with the help of heave limiter for all cases was $y_o = 0.573c$ (heave amplitude). However, as the system moves towards the heave limiter and with the help of the moment arm turns the hydrofoil in the opposite direction, it moves further down along the guide rod due to the inertia, with this procedure being repeated during the whole flapping cycle. Hence, with reference to figure 3(a), the actual heave amplitude is actually $y_{oac} = 0.671c$.

Figure 3(b) shows the time history of angular displacement. It is evident from the plot that the pitch motion of the hydrofoil is non-sinusoidal. The foil remains at its maximum pitching angle during the heave motion in between the two heave limiters, due to which the maximum angle remains constant for a given length in time as seen in figure 3(b). The time for which the angle remains constant is not equal for all pitching angle cases. This suggests that as the maximum pitching angle increases the time for which the maximum pitching angle remains constant (i.e. the time taken for the heave motion) decreases, indicating faster heave travel. When the foil reaches the end of its translational stroke, a stroke reversal occurs when the moment arm is in contact with the heave limiter. This is due to the test rig not having any elaborate mechanical system to enforce a fixed phase difference (ϕ) between pitch and heave motion or a particular motion profile. Due to the action of hydrodynamic forces on the passively oscillating foil, it was observed that the phase difference between pitch and heave was in the range of $50^\circ < \phi < 75^\circ$ in all cases.

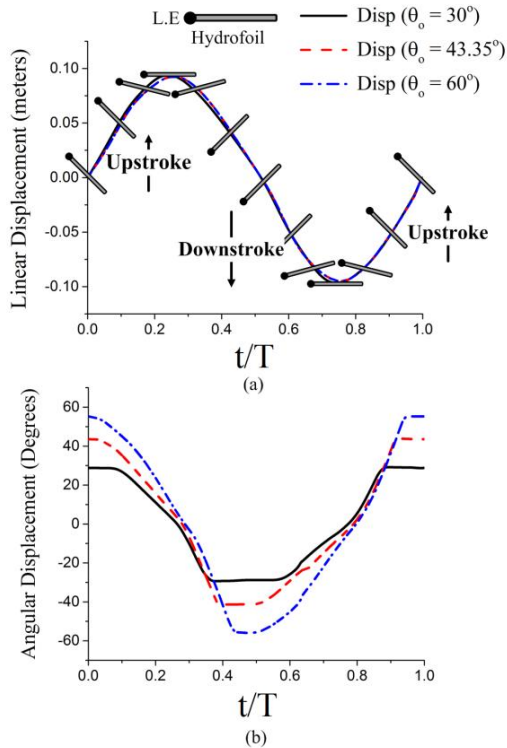


Figure 3. (a) Linear and (b) angular displacement time histories for $\theta_o = 30^\circ$, 43° and 60° at $U_o = 0.72$ m/s and 0.79 m/s.

Figure 4 shows phase-averaged vertical force ($F_{v-hydro}$) (figure 4 (a)) and moment ($T_{z-hydro}$) (figure 4 (b)) against non-dimensional time at both flow velocities. Ideally, the force and moment data would have a smooth profile with small variations, however due to the unsteadiness in the water flow and mechanical vibrations experienced by the test-rig, we observe large undulations in the force and moment results.

If compared with the kinematics data in figure 3, the results shown in figure 4 are in agreement with the physics involved in flapping foil energy harvesting, i.e., the lift must be in the same direction as the heave velocity and the foil rotates to its maximum prescribed pitch angle in the direction of heave motion (as shown in figure 2). It can be seen that the positive $F_{v-hydro}$ and $T_{z-hydro}$ are in the same time regime as the upstroke motion and the negative $F_{v-hydro}$ and $T_{z-hydro}$ (which is in the opposite direction) are also in the same time regime as the downstroke motion, hence confirming that energy is being transferred from the flow to the foil, causing the foil to passively move in a flapping fashion.

Figure 5 shows the variation of the power coefficient \bar{C}_p at $U_o = 0.72$ m/s and 0.79 m/s. It is seen that \bar{C}_p is not consistent throughout the whole flapping cycle due to the unsteadiness of hydrodynamic forces as shown in figure 4. However, in all cases the power extracted from the flow still shows a positive trend during the course of the flapping cycle. This is consistent with what we discussed earlier, that the power extracted is positive when the force directions are the same as the motions in most of the time during a flapping cycle.

Table 1 summarizes the mean power coefficient \bar{C}_p and power conversion efficiency η . $\theta_{o-max} = 43^\circ$ showed the highest \bar{C}_p and η than the other two pitch angles. A 30.5% increase alone was observed by just increasing the flow velocity showing an efficiency of 41% in energy extraction at $U_o = 0.79$ m/s. However, when the θ_{o-max} increased to 60° , the efficiency and average power coefficient dropped by 3% and 14%, respectively. This is also evident from figure 4 as the magnitudes of $F_{v-hydro}$ and $T_{z-hydro}$ of $\theta_{o-max} = 60^\circ$ is comparatively less than those at $\theta_{o-max} = 43^\circ$. However, \bar{C}_p and η are greater at $U_o = 0.79$ m/s than $U_o = 0.72$ m/s showing increases of 6% ($\theta_{o-max} = 30^\circ$), 30.52% ($\theta_{o-max} = 43^\circ$) and 11.5% ($\theta_{o-max} = 60^\circ$) in \bar{C}_p .

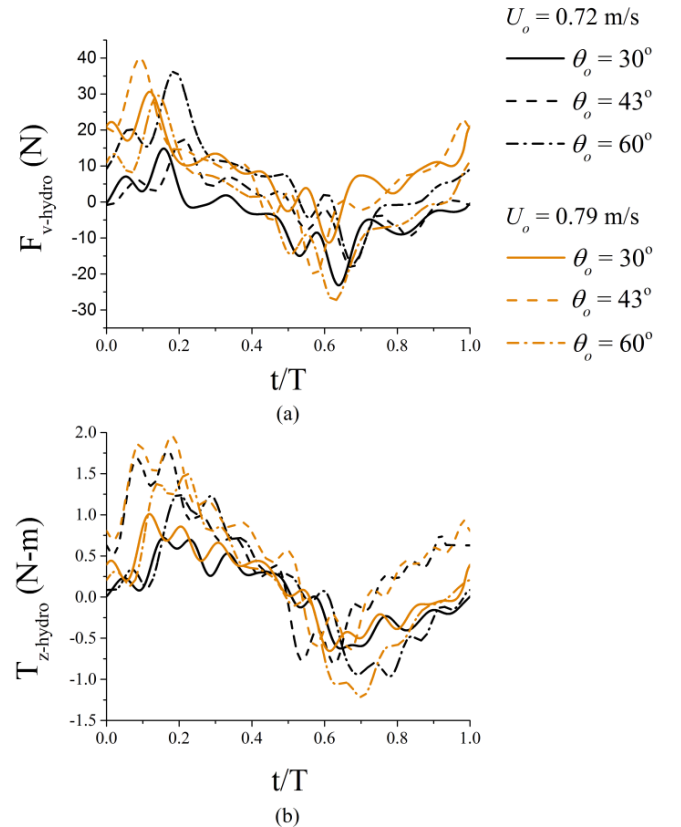


Figure 4. (a) $F_{v-hydro}$ for all angles of attack at $U_o = 0.72$ m/s and (b) $T_{z-hydro}$ for all angles of attack at $U_o = 0.79$ m/s.

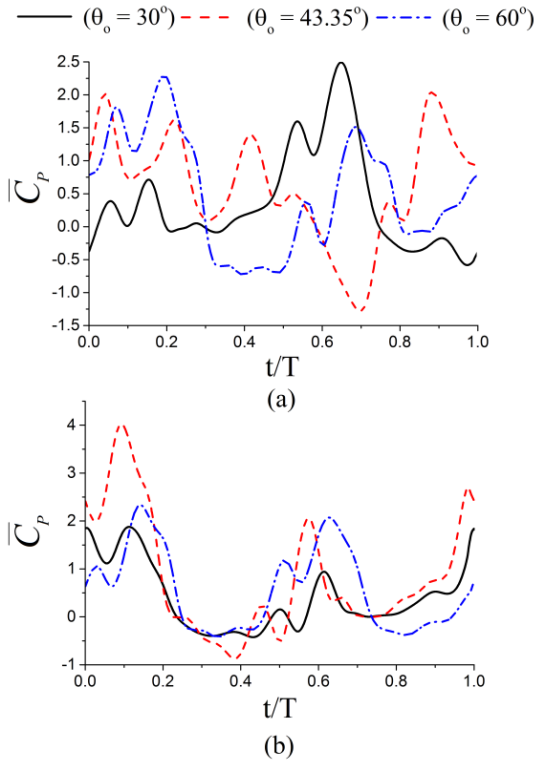


Figure 5. \bar{C}_p of (a) $\theta_o = 30^\circ, 43.35^\circ$ and 60° at $U_o = 0.72$ m/s and (b) $\theta_o = 30^\circ, 43.35^\circ$ and 60° at $U_o = 0.79$ m/s.

	Pitching Angle (θ_{o-max})	Flow Velocity (m/s)	\bar{C}_p	η (%)
(a)	30	0.72	0.367	21.55
		0.79	0.389	23.56
(b)	43	0.72	0.629	31.42
		0.79	0.821	41.02
(c)	60	0.72	0.539	28.15
		0.79	0.601	30.04

Table 1. Comparison of time averaged power coefficient and power conversion efficiency for $\theta_{o-max} = 30^\circ, 43^\circ$ and 60° at $U_o = 0.72$ m/s and 0.79 m/s.

Conclusion

This paper presents comparative analysis using time histories of kinematic and force/moment data, \bar{C}_p and η of a passively oscillating hydrofoil for three different pitching angles at two flow velocities. It was found that the flapping foil energy harvester demonstrated a non-sinusoidal pitching motion rather than a sinusoidal pattern as seen in most of the literature. This is due to the system not having any elaborate mechanical design to enforce any kind of prescribed motion pattern. Experimental data also revealed that the unsteady hydrodynamic forces acting on the flapping foil energy harvester imposed a phase difference in pitch and heave motions in the range $50^\circ < \varphi < 75^\circ$. It was also found that the hydrodynamic forces and moments were in the same direction with the velocities of the passively oscillating foil, indicating that the energy was indeed transferred from fluid to the foil. These results were further backed up by the \bar{C}_p data, which shows large-portion positive values during the course of the flapping cycle.

Results also indicate that by increasing the flow velocity, an increase in both \bar{C}_p and η with the pitch angle was observed in the investigated cases. $\theta_{o-max} = 43^\circ$ shows, on average a 35% increase in \bar{C}_p and 7% in η than at other pitch angles with the

highest η reaching 41% at $U_o = 0.79$ m/s, as values indicate in Table 1.

Future experiments planned include flow visualization and velocity field measurements using PIV coupled with real-time sensor data acquisition, which will help us fully understand how the associated vortex dynamics affects the hydrodynamic forces acting on a passively oscillating foil and its energy harvesting performance.

Acknowledgment

The first author of this paper, Mr. M. N. Mumtaz Qadri, would like to acknowledge the financial support from The Hong Kong Polytechnic University for his PhD study.

References

- [1] Ashraf M.A., Young J., Lai J.C.S., Platzer M.F., Numerical analysis of an oscillating wing wind and hydropower generator. *AIAA J* 2011; 49(7): 1374–1386 <http://dx.doi.org/10.2514/1.J050577>.
- [2] Fenercioglu I., Zaloglu B., Ashraf M.A., Young J., Lai J.C.S., and Platzer M.F., Flow around an Oscillating Tandem Wing Power Generator. *AIAA SciTech 53rd AIAA Aerospace Sciences Meeting*, 2015, <http://arc.aiaa.org/doi:10.2514/6.2015-1751>
- [3] Jones K. D. and Platzer M. F., Numerical computation of flapping-wing propulsion and power extraction *AIAA Meeting Papers*, 1997,97-0826
- [4] Jones K. D., Lindsey K. and Platzer M. F., An investigation of the fluid-structure interaction in an oscillating-wing micro-hydropower generator. *Fluid Structure Interaction II* (Southampton: WIT Press) 2003
- [5] Kinsey T. and Dumas G., Parametric study of an oscillating airfoil in a power-extraction regime *AIAA J*. 2008,**46** 1318–30
- [6] Kinsey T. and Dumas G., Computational fluid dynamics analysis of a hydrokinetic turbine based on oscillating hydrofoils *J. Fluids Eng.* 2012,**134** 021104
- [7] Kinsey T. and Dumas G., Optimal tandem configuration for oscillating-foils hydrokinetic turbine *J. Fluids Eng.* 2012,**134** 031103
- [8] McKinney W, DeLaurier J. Wingmill: an oscillating-wing windmill. *J Energy* 1981; 5(2): 109–115, <http://dx.doi.org/10.2514/3.62510>.
- [9] Platzer M.F. and Bradely Richard A., Oscillating wing power generator with flow induced pitch plunge phasing. *US Patent*, 2009, US2009/0121490
- [10] Semler Cogan S., Experimental investigation of an oscillating flow generator, *Dissertation Naval Postgraduate School*, 2010, <http://hdl.handle.net/10945/5425>
- [11] Shyy W, Liu H. Flapping wings and aerodynamic lift: the role of leading-edge vortices. *AIAA J* 2007; 45(12): 2817–2819, <http://dx.doi.org/10.2514/1.33205>.
- [12] Westwood, A., Ocean power wave and tidal energy review. *Refocus* 5, 50–55, 2004
- [13] Xiao Q., Liao W., Yang S. and Peng Y., How motion trajectory affects energy extraction performance of a biomimic energy generator with an oscillating foil? *Renew. Energy*, 2012, **37** 61–75
- [14] Zhu Q. and Peng Z., Mode coupling and flow energy harvesting by a flapping foil *Phys. Fluid*, 2009, **21** 033601